A bacterial size law revealed by a coarse-grained model of cell physiology

François Bertaux[1,2,3,4], Julius von Kügelgen[1], Samuel Marguerat[2,3,5], Vahid Shahrezaei[1,5]

1. Department of Mathematics, Imperial College London, London SW7 2AZ, UK
2. MRC London Institute of Medical Sciences (LMS), London W12 0NN, UK
3. Institute of Clinical Sciences (ICS), Faculty of Medicine, Imperial College London, London, W12 0NN, UK
4. Institut Pasteur and CNRS, C3BI - USR 3756, 25–28 Rue du Docteur Roux, 75015, Paris, France
5. To whom correspondence should be addressed

Abstract

Universal observations in Biology are sometimes described as “laws”. In *E. coli*, experimental studies performed over the past six decades have revealed major growth laws relating ribosomal mass fraction and cell size to the growth rate. Because they formalize complex emerging principles in biology, growth laws have been instrumental in shaping our understanding of bacterial physiology. Here, we discovered a novel size law that connects cell size to the inverse of the metabolic proteome mass fraction and the active fraction of ribosomes. We used a simple whole-cell coarse-grained model of cell physiology that combines the proteome allocation theory and the structural model of cell division. The model captures all available experimental data connecting the cell proteome composition, division size and growth rate in response to nutrient quality, antibiotic treatment and increased protein burden. Finally, a stochastic extension of the model explains non-trivial correlations observed in single cell experiments including the adder principle. This work provides a simple and robust theoretical framework for studying the fundamental principles of cell size determination in unicellular organisms.

Introduction

The behavior of complex biological systems can be described by surprisingly simple rules or “laws”, which connect quantitatively aspects of the cell composition with its physiology. Over the last six decades, the discovery of several rules, called the bacterial growth laws, transformed the field of microbial physiology (Schaechter et al. 1958; Dennis & Bremer 2008; Klumpp & Hwa 2014; Vadia & Levin 2015; Jun et al. 2018). Growth laws describe relationships between the exponential growth rate and cellular parameters. One such law states that the cellular ribosomal content is linearly dependent on the growth rate (we call this hereafter the first growth law). A second growth law states that average cell size is an exponential function of the growth rate (referred to hereafter as the second growth law). These laws formalize emerging relations between cellular processes quantitatively and therefore generate testable hypothesis for mechanistic studies of the molecular circuitry that underpin cell physiology (Hill et al. 2013; Scott et al. 2014).

What are the biological principles behind the first growth law? Theoretical and experimental studies identified constraints on cellular resource allocation as a key concept that explains many aspects of the first growth law. The theory of resource allocation describes how different groups of proteins with similar function (proteome sectors) are regulated reciprocally in conditions that affect growth rate. In particular, these studies showed that increased biosynthetic demand at higher growth rates underpins the positive correlation of the proteome fraction dedicated to ribosomal proteins with the growth rate. Interestingly, Hwa and co-workers (Scott et al. 2010) also showed that the first growth law breaks down for orthogonal modes of growth rate modulation, such as translation inhibition or overexpression of useless proteins. This indicates that increased burden on gene expression generates physiological states that feedback on growth in ways that are distinct from those induced by changes in nutrient quality. Based on these findings, they proposed a phenomenological model of proteome allocation that extended the first growth law to these orthogonal types of growth rate modulation (Scott et al. 2010). More mechanistic coarse-grained models predicting both the growth rate and the coarse-grained proteome as a function of growth conditions have also been proposed confirming and extending this finding (Marr 1991; Molenaar et al. 2009; Weisse et al. 2015; Maitra & Dill 2015; Bosdriesz et al. 2015; Maitra & Dill 2016; Pandey & Jain 2016; Giordano et al. 2016; Liao et al. 2017; Thomas et al. 2018; Sharma et al. 2018; Pandey et al. 2018).

In contrast, the mechanisms underlying the second growth law, which connects growth rate and cell size, are less well understood. In 1968, Donachie (Donachie 1968) proposed that an exponential dependency of cell size on growth rate indicated that: 1) the timing of DNA replication is fully controlled by cell size, and is triggered at a constant volume per origin of replication; 2) cell division is enslaved to the DNA replication processes, and occurs after a constant time-interval following replication initiation, which encompasses DNA replication and cell division (*C+D* period). However, while recent work has confirmed that DNA replication is strongly size-controlled (Wallden et al. 2016) and that the initiation size per origin is invariant across a large range of growth rates and types of growth rate modulations (Si et al. 2017), what determines the duration of the *C+D* period is still unclear. Moreover, the relationship between cell size and growth rate does not follow the second growth law, when burden on gene expression is increased or translation inhibited (Basan et al. 2015; Si et al. 2017). This indicates that duration of the *C+D* period is regulated in non-trivial ways outside of the canonical growth modulations based on nutrient quality. To date, unlike for the first growth law, mechanistic understanding of this phenomenon in connection to the second growth law is lacking.

The two growth laws discussed so far are based on average cell population measurements. However, the variations at the single cell level from the population average also provides rich and complementary insights into the biology of cell growth and division (Taheri-Araghi, Brown, et al. 2015; Kennard et al. 2016). Cells can control their size through a ‘sizer’ mechanism, where regardless of birth size they grow to an average size and then they divide. But, recent advances in single-cell techniques led to the discovery that bacterial cells achieve cell size homeostasis via an ‘adder’ principle, where cells add a constant size between birth and division independent of the birth size (Campos et al. 2014; Taheri-Araghi, Bradde, et al. 2015; Amir 2014). The adder phenomenon has

been observed in several bacteria, yeast, archea and mammalian cells (Iyer-Biswas et al. 2014; Taheri-Araghi, Brown, et al. 2015; Deforet et al. 2015; Soifer et al. 2016; Chandler-Brown et al. 2017; Logsdon et al. 2017; Eun et al. 2017; Priestman et al. 2017; Varsano et al. 2017; Cadart et al. 2018). Despite its broad conservation, the mechanistic basis of this phenomenon remains elusive and hotly debated. It has been suggested that the adder phenomenon is related to second growth law assuming that replication controls cell division (Ho & Amir 2015; Amir 2017). However, this model is challenged by recent studies that questioned the role of DNA replication in controlling division of single cells (Harris & Theriot 2016; Micali et al. 2018; Si et al. 2018).

Here, we present a coarse-grained model of bacterial physiology that unifies the proteome allocation theory with the structural model of division control (Fantes et al. 1975). With a small number of fitting parameters, the model captures a wide range of experimental measurements of protein mass fraction and cell size across growth conditions revealing a novel bacterial size law where cell size depends on the metabolism proteome sector mass fraction and the fraction of active ribosomes. This new law is simple and more general than the original second growth law. Finally, the model exhibits single cell properties that are consistent with experimental observations including the adder size control.

Results

A minimalistic whole-cell coarse-grained model to predict cell composition and cell size

We developed a minimalistic whole-cell coarse-grained mathematical model to predict cell composition, growth rate and cell size for at least three types of growth rate modulation: 1) change of nutrient quality, 2) translation inhibition by chloramphenicol and 3) forced expression of useless proteins. These modulations were selected because they have been instrumental in uncovering key principles of proteome allocation underpinning the first growth law (Scott et al. 2010) and have abundant experimental measurements available (Scott et al. 2010; Basan et al. 2015; Taheri-Araghi, Bradde, et al. 2015; Si et al. 2017).

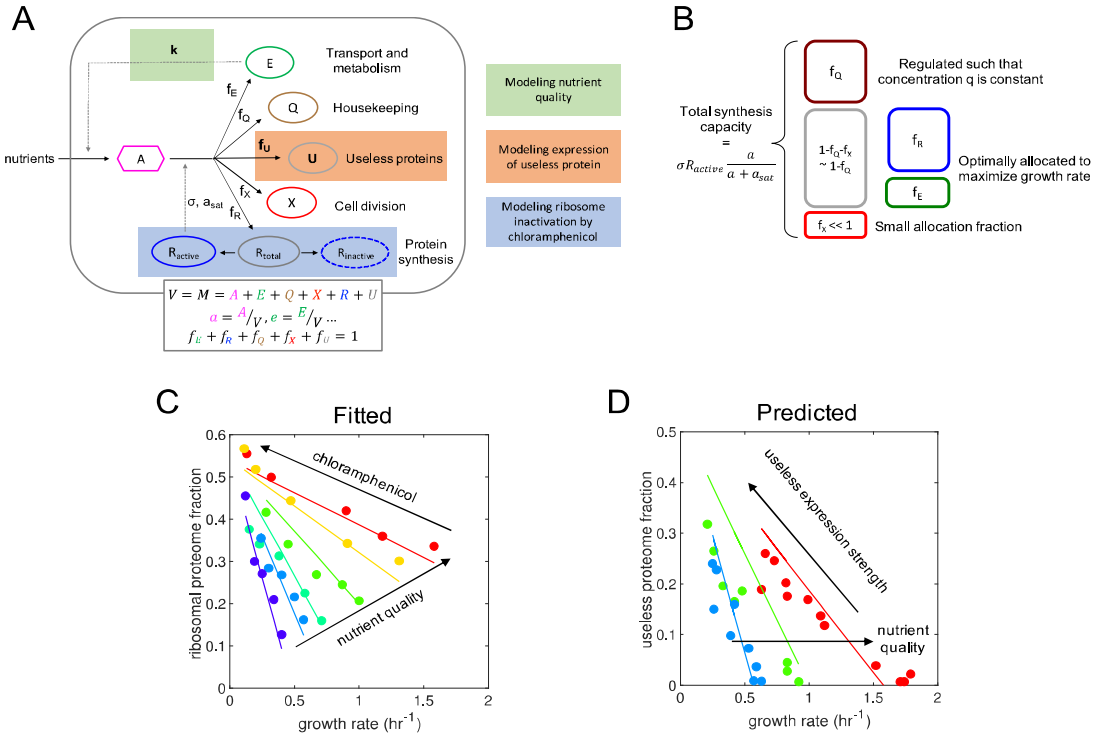

Figure 1. A simple whole-cell coarse-grained model of bacterial growth reproduces proteome allocation data. *(A) Schematic of model structure displaying model components (proteome sectors E, R, Q and X and protein precursor A) and reactions (metabolism, protein synthesis). How the three types of growth rate modulation (nutrient quality, expression of useless protein and ribosome inactivation) are modeled is also highlighted. See Main Text and Methods for details. (B) Allocation of total protein synthesis capacity between proteome sectors. The different allocation fractions* f_E, f_R *and* f_Q *are chosen such that the steady-state growth rate (see equations in Figure 2B) is optimized under the constraint that the concentration of housekeeping proteins Q is equal to a constant q. (C) Fitted model (*$\sigma = 6.69\ hr^{-1}$, $a_{sat} = 0.02$, $q = 0.454$*, see Supplementary Figure 1) quantitatively reproduces ribosomal proteome fraction data (Scott et al., 2010) for nutrient and chloramphenicol growth rate modulations. (D) Fitted model also predicts the relationship between growth rate and useless proteome fraction for forced expression of useless protein, which was not used in the fit (also from Scott et al., 2010).*

As in previous work, the model (Figure 1, see Methods for a mathematical description) considers only two types of molecular components: protein precursors (noted *A*) and proteins (Molenaar et al. 2009; Weisse et al. 2015; Pandey & Jain 2016). Proteins are split between four different classes (or sectors): transport and metabolism proteins (referred to as only metabolic sector for brevity) (*E*), ribosomal proteins (*R*), housekeeping proteins (*Q*), and division proteins (*X*). *E* proteins catalyse the import and transformation of external nutrients (not explicitly modelled) into precursors *A*. *R* proteins are involved in the synthesis of proteins from precursors. *Q* proteins are involved in cellular functions that do not directly contribute to growth. *X* proteins are regulating cell division (see below). Lastly, when growth rate is modulated by increased burden on gene expression, we consider an additional

class of “useless” proteins noted *U* (Figure 1). All proteins are stable in our model and only diluted by cell growth. The model enforces mass conservation, cell mass being defined as the sum of all molecular components. Finally, except for the import and transformation of nutrients into precursors, all reactions leave cell mass unchanged and assumes mass density homeostasis (cell volume and cell mass are therefore equivalent), as observed experimentally (Basan et al. 2015).

Finally, the model assumes that the protein synthesis allocation fractions of metabolic (f_E) and ribosomal proteins (f_R) are optimal for growth (Figure 1B) under the constraint that the concentration of housekeeping (*Q*) proteins must be equal to a fixed, condition-independent concentration *q*. We also assume that the synthesis allocation fraction to division proteins f_X is small. As a result, the steady-state cell composition depends only on: 1) three condition-independent parameters: the two ribosome biochemical parameters σ and a_{sat} and the housekeeping protein concentration q; and 2) three growth modulation parameters: the medium nutrient quality *k*, the chloramphenicol-imposed concentration of inactive ribosomes r_i, and the useless protein allocation fraction f_U.

The model reproduces quantitatively proteome allocation data (Scott et al. 2010) for the three types of growth modulation, by varying only 3 fitting parameters (Figure 1C; see Supplementary Figure 1 for details on the fitting procedure). Fitted values for σ and *q* (see caption of Figure 1) are highly consistent with previous estimates ($q \sim 0.45$ and $\sigma \sim 6\ hr^{-1}$, (Scott et al. 2010; Reuveni et al. 2017) When introducing useless proteins, the model also predicts useless protein fraction that is not included in the fitting (Figure 1D). Finally, our model uniquely takes into account the mass fraction of protein precursors (a). Notably, as suggested by Scott and colleagues, the fitted values of the ribosome enzymatic saturation constant a_{sat} and q are such that steady-state a values remain relatively small (below 15 %) while increasing with increasing nutrient quality (Scott et al. 2014).

Our model also explicitly includes cell division and assumes that it is triggered by the accumulation of proteins belonging to the *X* sector to an absolute copy number threshold (Figure 2A), as proposed before in the structural model (Fantes et al. 1975). This design enables prediction of changes in both cell size and coarse-grained cell composition as a function of cell growth. Note that we do not assume that *X* proteins are destroyed immediately after division. Altogether, our model assumptions result in simple and intuitive equations characterizing model steady-states (Figure 2B). Importantly, steady-state concentrations of cell components are not dependent on the cell cycle as expected under balanced growth and are valid when cell division is not modeled (as done for the fitting of the proteome fraction data above).

In summary, we have developed a whole-cell model of cell physiology that captures changes in proteome fractions as a function of growth rate while uniquely incorporating direct modeling of cell division control.

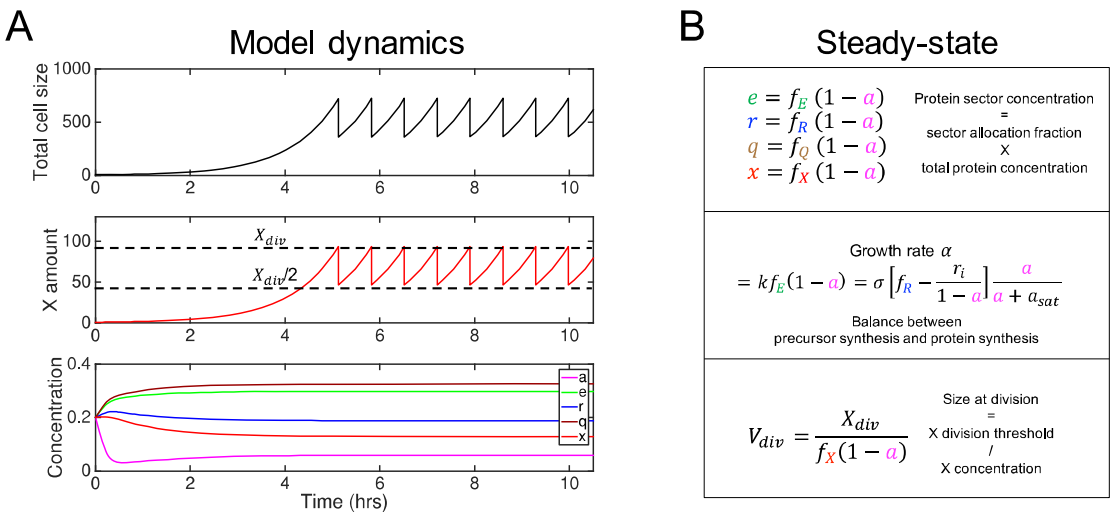

Figure 2. Integration of the structural model enables prediction of both cell composition and cell size. *(A) Simulation of model dynamics. After cell division (triggered when X number reaches X_{div}), cell content is partitioned equally among daughter cells and only one is followed ('mother machine' setting (Wang et al. 2010)). After a transient adaptation period, concentrations of cellular components are constant, cellular growth (size increase) is exponential and division occurs at a constant size. Here, nutrient quality is such that the growth rate is $1\ hr^{-1}$ and there is no chloramphenicol nor useless expression. (B) Equations characterizing model steady-state together with their intuitive interpretation (see Methods for their derivation). Those equations are used to find optimal allocation for given growth modulation parameters according to the principles described in Figure 1B. See Methods for details.*

Cell size can be predicted from coarse-grained cell composition across all conditions revealing a novel size law

Data from previous studies shows a complex relationship between cell size and growth rate across the three types of growth modulation (Figure 3B). Cell size increases with growth rate when nutrient quality is varied as posited by the second growth law, but the dependency on growth rate is inverted when growth rate is modulated by forced expression of useless proteins. Moreover, the impact of chloramphenicol-mediated translation inhibition on cell size appears to depend on the nutrient quality of the medium. We asked whether particular regulation of division proteins X by coarse-grained proteome sectors via the allocation fraction f_X could explain this complex pattern (Figure 3A).

We first considered a model whereby f_X follows the concentration of a single coarse-grained proteome sector only. Interestingly, size measurements for both nutrient quality and useless expression growth rate modulations are explained if f_X is set to follow the concentration (noted e, not to confuse with the mathematical constant) of the metabolic sector *E* exclusively (Figure 3D). However, this simple dependency cannot explain chloramphenicol-mediated translation inhibition data (Supplementary Figure 4A). We then considered dependencies of f_X on two coarse-grained proteome quantities. We found that when f_X depends on both the *E* sector concentration and the fraction of

active ribosomes (noted $\frac{r_a}{r}$, where r_a is the concentration of active ribosomes), the observed relationship between size and growth rate for all three types of growth rate modulation can be quantitatively captured (Figure 3C and 3E). Notably, the fitted exponent values are very close to 1 and -2/3 for e and $\frac{r_a}{r}$ respectively. Because f_X and cell size are directly linked ($V_{div} = \frac{X_{div}}{f_X(1-a)}$, see Figure 2B), it follows that cell size V scales with $e^{-1} \times (\frac{r_a}{r})^{2/3} \times (1-a)^{-1}$. The factor $(1-a)$ has in fact a minor contribution (Supplementary Figure 4-B,C,D). Based on this we propose a novel size law formalized as follows:

$$V \propto e^{-1} \times (\frac{r_a}{r})^{2/3}$$

In summary, our minimalistic model quantitatively captures how both size and coarse-grained cell composition change with the growth rate for all three types of growth modulation with only five parameters (σ, a_{sat}, q and the two exponents of the f_X dependency on e and r_a/r, those exponents being very close to 1 and -2/3 respectively). Therefore, *E. coli* cell size can be predicted from only two coarse-grained proteome quantities, metabolism sector concentration and the fraction of active ribosomes leading to the definition of a novel growth law. While our model uses the structural model of cell division to connect cell size and coarse-grained cell composition, the resulting size law is valid as a phenomenological relationship whether or not the structural model of cell division is valid (Supplementary Figure 4D).

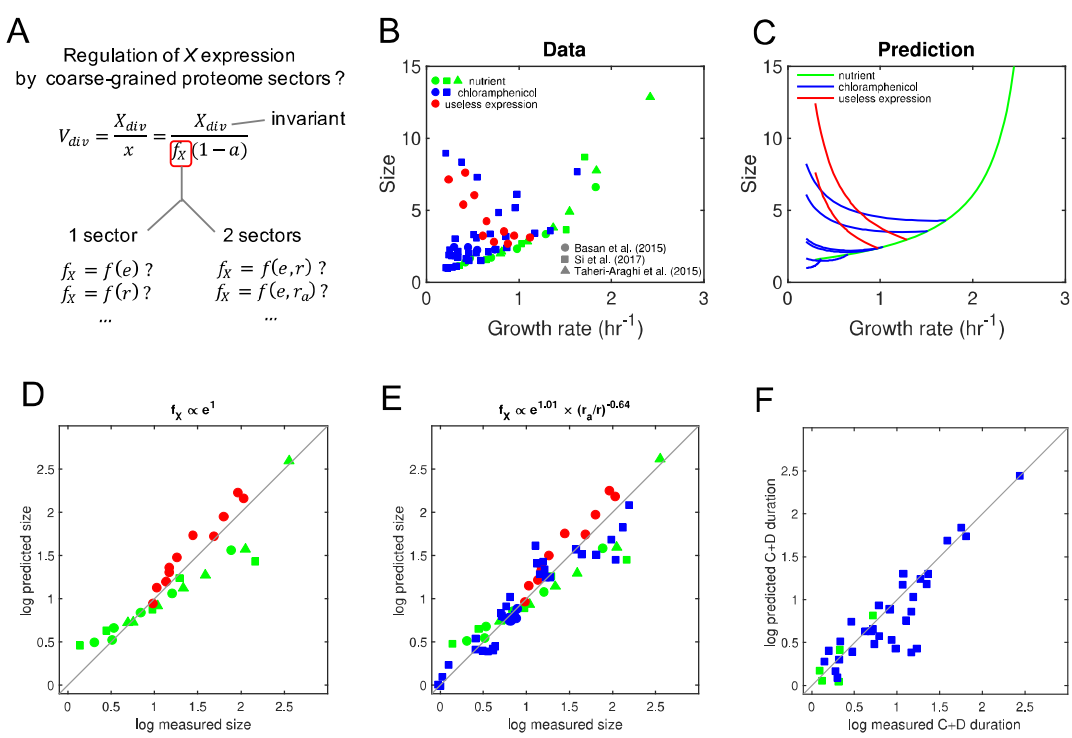

Figure 3. Regulation of division proteins by two proteome sectors quantitatively explain cell size across growth modulations. *(A) Hypothesis stating that X expression could depend on the*

concentration of one or two coarse-grained proteome sectors. Here we assume that X_{div} is invariant. (B) Empirical relationship between cell size and growth rate for three types of growth rate modulation (nutrient quality, chloramphenicol-mediated translation inhibition and expression of useless protein). Data aggregated from three studies, Basan et al. (2015), Si et al. (2017) and Taheri-Araghi et al. (2015). A scaling factor for size was applied on Si et al. and Taheri-Araghi et al. data to make the nutrient modulation data of the three studies consistent (see Supplementary Figure 2). (C) Predicted relationship between cell size and growth rate when X expression depends on both E concentration and the fraction of active ribosomes. (D) Regulation of X expression by E alone could explain size data for nutrient modulation and useless expression modulation (middle), but not chloramphenicol-mediated translation inhibition (Supplementary Figure 4A). (E) Among possible regulations of X by two coarse-grained quantities, regulation by E concentration and the fraction of active ribosomes explains size data for all three types of growth rate modulations (this regulation model was used for (C)). (F) Predicted C+D durations agree with measurements by Si et al. (2017). C+D is predicted by $C + D = \frac{log[V_{div}/S_0]}{\alpha}$, where α is the growth rate, V_{div} is the model-predicted size (3C and 3E) and S_0 is a constant measured in Si et al. (2017).

Emergence of 'adder' size homeostasis and cellular individuality in the presence of noise

So far, we have neglected cell-to-cell variability and focused on predicting average cell composition, size and growth rate at steady-state as a function of growth conditions. However, isogenic cells growing in a constant environment show significant phenotypic variability, notably for global traits such as growth rate or division size (Elowitz et al. 2002; Levine & Hwa 2007; Taheri-Araghi, Bradde, et al. 2015). Moreover, non-trivial correlations between single-cell traits are often observed and contain rich information about regulatory mechanisms (Dunlop et al. 2008; Amir 2014; Kiviet et al. 2014; Taheri-Araghi, Bradde, et al. 2015; Kennard et al. 2016; Kleijn et al. 2018; Thomas et al. 2018; Pandey et al. 2018). Since our model is based on biochemical reactions between coarse-grained molecular components, dynamic cell-to-cell variability naturally emerges when adopting a stochastic interpretation of all reactions and random partitioning of components at division (Figure 4A).

In the deterministic model, the two parameters X_{div} (the number of division molecules X needed to trigger cell division) and f_X^{scale} (the constant factor in the dependency of f_X on the coarse-grained proteome) are only setting the size scale via their ratio (see Figure 3A). In the presence of reaction noise, those parameters will now impact the extent of cell-to-cell variability in growth rate and in size at division. Even with this simple model of gene expression noise, we could find values of those two parameters that lead to realistic estimates of both noise in growth rate and size at birth (according to mother machine data across nutrient conditions, (Taheri-Araghi, Bradde, et al. 2015), Supplementary Figure 5).

Stochastic simulations of our model lead to a near 'adder' size homeostasis, as observed experimentally (Figure 4B, red circles). Deviation towards 'sizer' size homeostasis (observed experimentally at very slow growth, (Wallden et al. 2016)) could also be recovered with minor model

modifications, namely by introducing a constant degradation rate of X during the cell cycle (Figure 4B, blue squares). We also explored the relationship between cell size at birth and cellular growth rate across the three types of growth rate modulation (Figure 4C). This relationship is known to deviate from the one connecting average size at birth and average growth rate when conditions are varied (Taheri-Araghi, Bradde, et al. 2015; Kennard et al. 2016). Strikingly, those were clearly captured by our model (Figure 4C).

In summary, our minimalistic coarse-grained model generates realistic cell-to-cell variability in growth rate and cell size, as well as realistic correlations between added size and birth size ('adder' size homeostasis) and between growth rate and birth size.

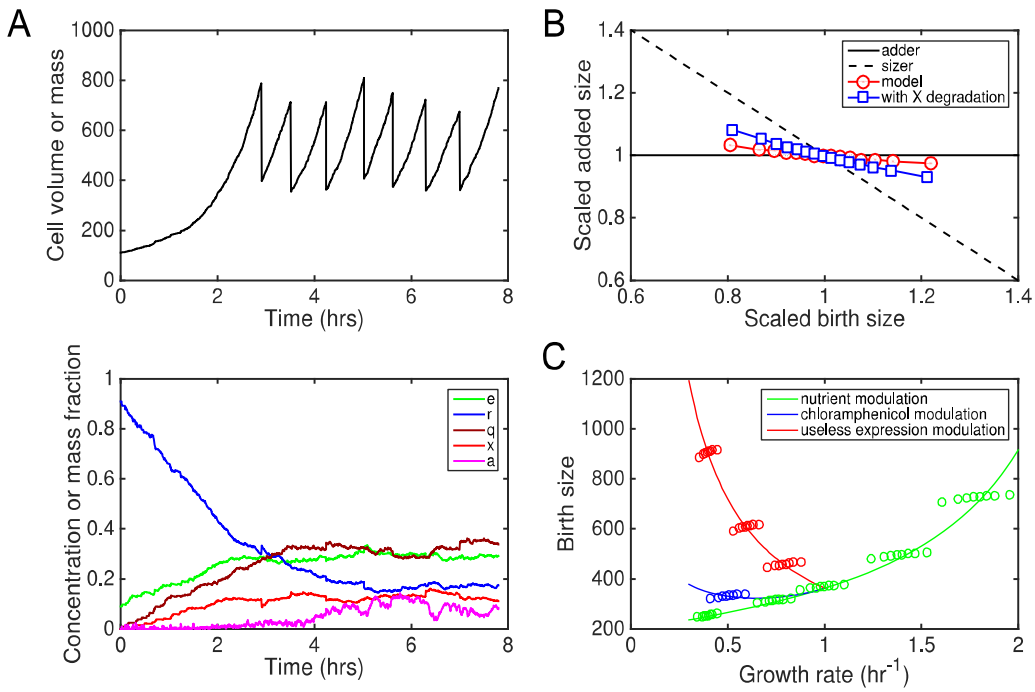

Figure 4. Emergence of 'adder' size homeostasis and cellular individuality in the presence of reaction noise. *(A) Simulation of model dynamics with molecular noise (top: total cell size, bottom: concentrations of cellular components). At division, cellular components are randomly split between daughter cells, so the tracked daughter has a probability* $1/2$ *of getting each mother cell component. Same parameters as in Figure 2A. The parameters* X_{div} *and* f_X^{scale} *were chosen to obtain realistic cell-to-cell variability in size at birth and growth rate (see Supplementary Figure 5). (B) Model leads to near 'adder' size homeostasis. Average added size during one cell cycle as a function of birth cell size (via binning) is plotted. The very weak deviation towards 'sizer' can be explained by a residual correlation between size at birth and X count at birth due to the non-zero share of X in total size. A model variant where* X *is actively degraded at a constant rate and displaying a stronger deviation towards 'sizer' behavior is also shown. Other model variants exploring size homeostasis properties are discussed in Supplementary Figure 7. (C) Emergence of cellular individuality. The dependence of individual cell birth size with their cellular growth rate in given growth conditions is distinct from the*

dependence of average birth size on average growth rate when growth conditions are varied, as observed experimentally (see for instance Taheri-Araghi et al., 2015).

Discussion

In this work, we have proposed a simple and minimalistic whole-cell coarse-grained model of *E. coli* physiology to predict the relationship between growth rate, cell composition and cell size for three different types of growth rate modulation (Figure 1A and Figure 2). Our model unifies previous efforts to understand proteome allocation (Molenaar et al. 2009; Scott et al. 2010; Scott et al. 2014; Weisse et al. 2015; Pandey & Jain 2016) and division control (Fantes 1977; Taheri-Araghi, Bradde, et al. 2015; Basan et al. 2015; Ghusinga et al. 2016). While other theoretical models (Scott et al. 2010; Scott et al. 2014; Weisse et al. 2015; Pandey & Jain 2016) have also captured proteome allocation data, our model stands out because: 1) it uses a minimal set of parameters (similar to the 'rheostat' model, (Scott et al. 2014)); 2) it is holistic with respect to cell composition and cell size; 3) it does not neglect the mass fraction of protein precursors. Despite its simplicity and low parameter number, our model quantitatively reproduces experimental data on proteome allocation (Figure 1B) and average cell size (Figure 3C) for the three types of growth rate modulation (change of nutrient quality, chloramphenicol-mediated ribosome inactivation and expression of useless proteins). In addition, when reaction noise is included in the model, experimental observations such as the *adder* principle of size homeostasis and non-trivial correlations between cellular growth rate and cell size are predicted (Figure 4).

A remarkable result of our study is the emergence of a novel size law related to the second growth law. This law states that only one coarse-grained quantity characterizing cell composition is sufficient to predict quantitatively cell size changes in response to nutrient quality and to over-expression of a useless protein (Figure 3C and 3E, Supplementary Figure 4). A second coarse-grained quantity is required for prediction of cell size when translation is inhibited. Those quantities are the mass fraction (or equivalently, concentration) of metabolic proteins (*e* in the model) and the fraction of total ribosomes that are active (r_a/r), respectively. Strikingly, best fit is robustly obtained for exponent values close to ~ -1 for the metabolic protein concentration and $\sim 2/3$ for the fraction of active ribosomes. We did not impose constraints on the values of exponents when fitting size data, the fact that fitted exponents are close to such particular values is therefore remarkable and suggests a fundamental underlying physical mechanism. This results in a novel 'size law' stating: $V \propto e^{-1} \times (\frac{r_a}{r})^{2/3}$. In the absence of translation inhibition and at intermediate to fast growth the fraction of active ribosomes is close to 1 (Dai et al. 2016), therefore the law reduces to the simple form $V \propto e^{-1}$. This 'size law' is very different in nature from the second growth law stating that $V \propto \exp[\alpha(C + D)]$, where α is the growth rate, C the duration of DNA replication and D the duration between end of DNA replication and cell division. By construction, the second growth law links size at division to the control of DNA replication by size (Donachie 1968; Wallden et al. 2016; Amir 2017). It predicts a simple exponential dependency with growth rate for nutrient quality modulation because those three quantities are largely independent of growth rate. However, while average size per origin at replication

initiation is invariant across a wide range of growth conditions, both C and D durations change with growth conditions in complex ways (Si et al. 2017). Therefore, the second growth law is replication-initiation-centric and of limited use to make predictions on cell size at division outside of the canonical type of growth rate modulation (change in nutrient quality). In contrast, the 'size law' we propose directly links coarse-grained cell composition to cell size and it explains the observed variation in the C and D durations at least across three different types of growth rate modulation. This law can generate directly testable predictions, such as cell size and *C+D* durations for growth modulations involving both gene expression burden and translation inhibition by chloramphenicol.

In agreement with our results, recent studies contradict the replication-initiation-centric view of cell size control (Amir 2017). Based on single-cell correlation statistics, Micali and colleagues (Micali et al. 2018) propose that two concurrent processes, each controlling DNA replication and division, co-determine the effective size at division. Furthermore, Si and colleagues (Si et al. 2018) experimentally demonstrated that two independents 'adders' homeostasis mechanisms are in place for DNA replication initiation and cell division. This does not mean that cellular constraints related to DNA replication are not affecting average cell size at division. Yet it indicates that cell division is not enslaved to the process controlling DNA replication initiation. Also, recent experiments reported different amounts of DNA in newborn cells, suggesting the chromosome is not involved in size homeostasis or responsible for the adder behavior (Huls et al. 2018). Here we find that homeostatic properties at the level of cell division appear consistent with the structural model of division control. As shown in Figure 4, the structural model implemented at the single cell level recovers 'adder' size control (Ghusinga et al. 2016), deviation towards 'sizer' (Wallden et al. 2016) in some parameter regimes (Supplementary Figure 7) and non-trivial deviations from growth law at the single cell level (Taheri-Araghi, Bradde, et al. 2015; Kennard et al. 2016). We note that as suggested by a recent model (Micali et al. 2018), there could be still a role for DNA-replication or segregation in division control, for example when these processes are slowed down (Si et al. 2017; Deforet et al. 2015).

In our model, quantitative mapping between cell composition and cell size is realized via a dependency of the division protein X allocation fraction on e and $\frac{r_a}{r}$ (Figure 3A), but it is also valid on its own as a phenomenological observation (Supplementary Figure 4). What could explain the quantitative link between the coarse-grained quantities e and $\frac{r_a}{r}$ and cell size? Under the structural model of division control, a further assumption that the division threshold X_{div} is invariant across conditions, would imply that the X allocation fraction f_X scales with e and the inverse of $(\frac{r_a}{r})^{2/3}$. However, under the same assumption that X_{div} is invariant, Basan and colleagues (Basan et al. 2015) could not identify in proteomics data candidate proteins whose proteome fraction is behaving quantitatively as you would expect for the factor X (given their cell size data). This result suggests that there is no single protein triggering division when reaching a fixed, condition-independent amount. A simple possibility given our results is that X follows exactly the relative abundance of metabolic proteins E, while the division threshold X_{div} scales with the fraction of active ribosomes to the power $2/3$.

Other constraints could explain a condition-dependent threshold X_{div}. One attractive possibility is that constraints related to cell geometry are playing a role, as proposed recently (Harris & Theriot 2016). For example, it is possible that resource allocation that maximize growth sets a balance between surface and cytoplasmic proteins that constrains the surface-to-volume ratio (i.e. width for rod-shaped cells). In turn, depending on the mechanism 'counting' the absolute amount of *X* molecules, the threshold can depend on width. In the context of a width-dependent threshold, as suggested by several studies *FtsZ* is an attractive candidate as the sole *X* factor (Palacios et al. 1996; Harris & Theriot 2016; Zheng et al. 2016; Si et al. 2018).

In this work, we have tried to explain the mechanistic origin of size regulation across growth conditions. Whether this is an evolved trait that optimizes fitness is a more difficult question. While size changes due to expression of useless proteins or translation inhibition by drugs may not be an evolved trait, the increased size with nutrient modulation of growth rate seems to be a universal property of microbes, which makes it likely to be an evolved property of unicellular systems (Turner et al. 2012; Chien et al. 2012). In a recent *in silico* study, we showed that increased size at fast growth prevents an increase in gene expression noise for proteins with decreasing concentrations (Bertaux et al. 2018). Metabolic proteins *E* are such proteins, and noise in their expression is likely detrimental to fitness. Interestingly, the inverse relationship between cell size and metabolic protein concentration e found in this study implies that the total number of metabolic proteins is kept constant across growth conditions. This raises the possibility that the evolution of size regulation in response to growth conditions has been driven by selective pressures acting on metabolic protein expression noise rather than on size directly. Testing fitness benefit of size regulation is difficult (Zheng et al. 2016; Monds et al. 2014) but should ultimately shed light on the constraints that shaped its evolution.

Modelling cellular systems by considering the cellular context within which they operate is fundamental to a full mechanistic understanding of their function. Modelling has shown that function of simple synthetic networks can be affected by cell cycle and cell growth, when cell physiology and resource allocation is taken into account (Klumpp & Hwa 2014; Weisse et al. 2015; Borkowski et al. 2016; Bertaux et al. 2018). The current study illustrates that integrating coarse-grained models of cell physiology with simple models of division control could reveal novel size law providing a link between cell size and cellular resource allocation. Overall, our study highlights the importance of systematic integration of whole-cell physiological models in the study of natural and synthetic cellular systems.

Acknowledgements

We would like to thank Suckjoon Jun, Istvan Kleijn, Guillaume Le Treut, Peter Sarkies, Fangwei Si, Peter Swain and Philipp Thomas for feedback on our manuscript and members of the Marguerat and Shahrezaei groups for discussions. F.B. received financial support from Leverhulme Research Project Grant (RPG-2014-408) awarded to S.M. and V.S. S.M. is supported by the UK Medical Research Council.

Methods

Model reactions

Our model considers the following reactions between coarse-grained cell components:

$\emptyset \xrightarrow{kE} A$ (nutrient import and transformation into protein precursors)

$A \xrightarrow{f_E\, \sigma\,(R-r_iV)\,\frac{a}{a+a_{sat}}} E$ (synthesis of *E* proteins)

$A \xrightarrow{f_R\, \sigma\,(R-r_iV)\,\frac{a}{a+a_{sat}}} R$ (synthesis of *R* proteins)

$A \xrightarrow{f_Q\, \sigma\,(R-r_iV)\,\frac{a}{a+a_{sat}}} Q$ (synthesis of *Q* proteins)

$A \xrightarrow{f_X\, \sigma\,(R-r_iV)\,\frac{a}{a+a_{sat}}} X$ (synthesis of *X* proteins)

$A \xrightarrow{f_U\, \sigma\,(R-r_iV)\,\frac{a}{a+a_{sat}}} R$ (synthesis of *U* proteins)

Where the cell volume is $V = E + R + Q + X + U + A$, the protein synthesis allocation parameters $(f_E, f_R, \ldots)$ respect $f_E + f_R + f_Q + f_X + f_U = 1$, and $a = \frac{A}{V}$ (we will also note *e*, *r*, *q*, *x*, *u*, … the concentrations *E/V*, *R/V*, etc…). The parameter k is the medium nutrient quality, r_i is the chloramphenicol-imposed concentration of inactive ribosomes and f_U is the imposed allocation fraction of useless proteins. The parameter σ is the maximal rate of protein synthesis by one ribosome and a_{sat} is the enzymatic saturation constant of ribosomes. Note that all protein synthesis reactions conserve mass, so that $\frac{dV}{dt} = kE$.

Differential equations

A deterministic interpretation of these reactions leads to the following set of differential equations for absolute amounts of coarse-grained cell components:

$$\frac{dA}{dt} = kE - \sigma(R - r_iV)\frac{a}{a + a_{sat}}$$

$$\frac{dE}{dt} = f_E\, \sigma(R - r_iV)\frac{a}{a + a_{sat}}$$

$$\frac{dR}{dt} = f_R\, \sigma(R - r_iV)\frac{a}{a + a_{sat}}$$

$$\frac{dQ}{dt} = f_Q\, \sigma(R - r_iV)\frac{a}{a + a_{sat}}$$

$$\frac{dX}{dt} = f_X\, \sigma(R - r_iV)\frac{a}{a + a_{sat}}$$

$$\frac{dU}{dt} = f_U\, \sigma(R - r_i V) \frac{a}{a + a_{sat}}$$

These differential equations are used to simulate Figure 2A, together with the halving of all amounts at division, which is triggered when $X = X_{div}$.

The above differential equations can be also written in terms of concentrations, noticing that $\frac{dV}{dt} = kE = k\,e\,V$:

$$\frac{da}{dt} = ke - \sigma(r - r_i) \frac{a}{a + a_{sat}} - kea$$

$$\frac{de}{dt} = f_E\, \sigma(r - r_i) \frac{a}{a + a_{sat}} - ke^2$$

$$\frac{dr}{dt} = f_R\, \sigma(r - r_i) \frac{a}{a + a_{sat}} - ker$$

$$\frac{dq}{dt} = f_Q\, \sigma(r - r_i) \frac{a}{a + a_{sat}} - keq$$

$$\frac{dx}{dt} = f_X\, \sigma(r - r_i) \frac{a}{a + a_{sat}} - kex$$

$$\frac{du}{dt} = f_U\, \sigma(r - r_i) \frac{a}{a + a_{sat}} - keu$$

In the above equations, the last terms represent dilution by cell growth. Because concentrations are conserved at division, their dynamics and steady-state values are independent of the division threshold X_{div}.

Steady-state growth

In this model, steady-state growth (or balanced growth, i.e. steady concentrations of coarse-grained cell components) is necessarily exponential at rate $\alpha = k\,e$, because $\frac{dV}{dt} = kE = k\,e\,V$. By setting the time derivatives to zero, we obtain the following equations constraining the steady-state cell composition (*e*,*r*,*q*,*x*,*u*,*a*):

$$ke(1 - a) = \sigma(r - r_i) \frac{a}{a + a_{sat}}$$

$$ke^2 = f_E\, \sigma(r - r_i) \frac{a}{a + a_{sat}}$$

$$ker = f_R\, \sigma(r - r_i) \frac{a}{a + a_{sat}}$$

$$keq = f_Q\, \sigma(r - r_i) \frac{a}{a + a_{sat}}$$

$$kex = f_X\,\sigma(r - r_i)\frac{a}{a + a_{sat}}$$

$$keu = f_U\,\sigma(r - r_i)\frac{a}{a + a_{sat}}$$

The first equation gives another expression for the growth rate: $\alpha = \sigma\frac{r-r_i}{1-a}\frac{a}{a+a_{sat}}$, where the factor $\frac{r-r_i}{1-a}$ is in fact the proteome fraction of active ribosomes f_{RA}. We call r_a the mass fraction of active ribosomes $r - r_i$.

Combining the first equation with every other enable to express protein concentrations as a function of $(1 - a)$:

$e = f_E(1 - a)$, $r = f_R(1 - a)$, $q = f_Q(1 - a)$ and $x = f_X(1 - a)$

This is intuitive: a proteome sector concentration is equal to its allocation fraction times the total protein concentration $1 - a$.

Finally, plugging the latter into the first equation, we obtain an implicit equation for *a*:

$$kf_E(1 - a) = \sigma\left[f_R - \frac{r_i}{1 - a}\right]\frac{a}{a + a_{sat}}$$

This equation is also intuitive: it reflects the necessary balance between the rate of nutrient import and transformation into precursors and the rate of total protein synthesis.

Optimal proteome allocation fractions

So far the proteome allocation fractions f_E, f_R, f_Q, f_X and f_U were treated as parameters. To determine their values as a function of growth conditions, we assume that they are regulated so that steady-state growth rate is maximal under the constraint that the concentration of housekeeping proteins q is equal to a fixed, condition-independent constant. Furthermore, f_U is imposed by the induction level of the useless proteins, and we assume that $f_X << 1$.

It is possible to enumerate all possible steady-states respecting the imposed constraints, for example by varying a between 0 and $a_{max} = 1 - \frac{q+r_i}{1-f_U}$ (a_{max} is the limit case when $a + q + r_i + u = 1$, for higher values of a, constraints on cell composition cannot all be respected). Indeed, when a is fixed, there is a unique set of allocation fractions f_E, f_R and f_Q respecting steady-state and all constraints. Our algorithm to find the optimal allocation fractions and the corresponding cell composition is therefore as follows:

- for a given a in $[0,1 - \frac{q+r_i}{1-f_U}]$, find the unique solution $f_Q(a), f_E(a)$ and $f_R(a)$ with the following computations:
  - $f_Q = \frac{q}{1-a}$
  - $f_E + f_R = 1 - f_Q - f_U$

– $f_E = \frac{\left(f_E + f_R - \frac{r_i}{1-a}\right)\frac{\sigma}{k}\frac{1}{1-a}\frac{a}{a+a_{sat}}}{1+\frac{\sigma}{k}\frac{1}{1-a}\frac{a}{a+a_{sat}}}$

- the growth rate α is then given by $\alpha(a) = k f_E (1-a)$
- find the a maximizing α by bounded scalar optimization on a (using *MATLAB* function *fminbnd*)

Fitting σ, q and a_{sat} to proteome allocation data

The data is taken from Scott and colleagues (Scott et al. 2010). It consists of steady-state ribosome proteome fractions for a combinations of nutrient conditions and chloramphenicol concentrations (measured via the RNA/protein ratio, see (Scott et al. 2010) for justification).

To evaluate how well one parameter set (σ, q and a_{sat}) can explain this data, we first use the growth rate data for different nutrient conditions in absence of chloramphenicol to find the corresponding values of nutrient qualities (*k*) using simple scalar optimization. This leads to predictions for cell composition (including the ribosome mass fraction) for those nutrient conditions. Then, for each chloramphenicol perturbation data point, we search for the value of inactive ribosomes concentration (r_i) that leads to the observed growth rate reduction using simple scalar optimization. This leads to predictions for cell composition for all other data points. The goodness of fit is then taken as the mean square error between observed and predicted ribosome mass fractions.

To search for the best possible parameter sets, we employ a brute force approach by exploring a 3D cube in the parameter space (using the Sobol sequence algorithm (Sobol 1967) for varying σ and q within slices of constant a_{sat}, see Supplementary Figure 1). We exclude the parameter sets leading to a maximum growth rate (when *k* is infinitely large) below 15 minutes to avoid unrealistic parameterizations.

Finding regulation of f_X expression explaining cell size data across types of growth rate modulation

The structural model of cell division links the steady-state cell composition and cell division size via the concentration x of X proteins: $V_{div} = \frac{X_{div}}{x} = X_{div}\frac{1}{f_X(1-a)}$.

To search for regulation of f_X explaining cell size data across the three types of growth rate modulations, we considered the following form of f_X: $f_X \propto c_1^{\beta_1} c_2^{\beta_2}$ where $c_{1,2}$ are quantities depending on the coarse-grained cell composition and $\beta_{1,2}$ are exponents.

We considered the following coarse-grained quantities: coarse-grained concentrations e, r, r_a and a, allocation fractions f_R, f_E and f_Q, and the fraction of active ribosomes $\frac{r_a}{r}$ (not to confuse with the mass fraction of active ribosomes r_a or the proteome fraction of active ribosomes $f_{RA} = \frac{r-r_i}{1-a}$).

Fitting was performed using multilinear regression on the logarithm of cell size data using *MATLAB* function *regress*. Cell size data between different datasets was normalized as detailed in Supplementary Figure 2.

To estimate the *C+D* duration directly from our size estimate, we use the value of 'unit cell' or DNA replication initiation volume from (Si et al. 2017) ($S_0 = 0.28\,\mu m^3$, converted to the normalized size scale described in Supplementary Figure 2).

Stochastic model

The stochastic version of the model was simulated using the *Gillespie* algorithm and in a mother machine setting. When *X* reaches the division threshold X_{div}, each coarse-grained molecule is kept in the daughter cell that we keep simulating with probability ½. Note that we are modeling protein synthesis with a single reaction for each sector, hence abstracting away transcription and mRNA degradation. To simulate conditions where chloramphenicol is present, the model structure was modified for explicit modeling of ribosome inactivation and re-activation:

$$R_{active} \rightarrow k_b R_{inactive}$$

$$R_{inactive} \rightarrow k_u R_{active}$$

Where k_u is the rate of re-activation of chloramphenicol-inactivated ribosomes (constant) and k_b is the rate at which active ribosomes are inactivated by chloramphenicol (it depends on the concentration of chloramphenicol). We detail in Supplementary Figure 6 the choice of k_u and show that the average behavior of the stochastic model is consistent with the deterministic model.

Note that while for solving optimal proteome allocation the contribution of f_X is neglected, f_X is non-zero to guarantee finite cell size. To strictly ensure mass conservation in the dynamic model simulations (see Figure 2A and 4), we decreased the f_Q computed from optimal proteome allocation when neglecting f_X by the value of f_X imposed by the fitting of X_{div} and f_X^{scale} to data on cell size noise and growth rate noise (see Supplementary Figure 5).

Code availability

All the code for solving model steady-state, simulating model dynamics, parameter fitting, etc. as well as the scripts generating all figures is available on *GitHub*. It is written in *MATLAB* except the stochastic simulation code written in *C++*.

References

Amir, A., 2014. Cell Size Regulation in Bacteria. *Physical review letters*, 112(20).

Amir, A., 2017. Is cell size a spandrel? *eLife*, 6, p.18261.

Basan, M. et al., 2015. Inflating bacterial cells by increased protein synthesis. *Molecular Systems Biology*, 11(10), p.836.

Bertaux, F., Marguerat, S. & Shahrezaei, V., 2018. Division rate, cell size and proteome allocation: impact on gene expression noise and implications for the dynamics of genetic circuits. *Royal Society Open Science*, 5(3), pp.172234–19.

Borkowski, O. et al., 2016. Overloaded and stressed: whole-cell considerations for bacterial synthetic biology. *Current opinion in microbiology*, 33, pp.123–130.

Bosdriesz, E. et al., 2015. How fast-growing bacteria robustly tune their ribosome concentration to approximate growth-rate maximization. *The FEBS journal*, 282(10), pp.2029–2044.

Cadart, C. et al., 2018. Size control in mammalian cells involves modulation of both growth rate and cell cycle duration. *Nature communications*, 9(1), p.3275.

Campos, M. et al., 2014. A constant size extension drives bacterial cell size homeostasis. *Cell*, 159(6), pp.1433–1446.

Chandler-Brown, D. et al., 2017. The Adder Phenomenon Emerges from Independent Control of Pre- and Post-Start Phases of the Budding Yeast Cell Cycle. *Current biology : CB*, 27(18), pp.2774–2783.e3.

Chien, A.-C., Hill, N.S. & Levin, P.A., 2012. Cell size control in bacteria. *Current biology : CB*, 22(9), pp.R340–9.

Dai, X. et al., 2016. Reduction of translating ribosomes enables Escherichia coli to maintain elongation rates during slow growth. *Nature Microbiology*, 2, p.16231.

Deforet, M., van Ditmarsch, D. & Xavier, J.B., 2015. Cell-Size Homeostasis and the Incremental Rule in a Bacterial Pathogen. *Biophysical journal*, 109(3), pp.521–528.

Dennis, P.P. & Bremer, H., 2008. Modulation of Chemical Composition and Other Parameters of the Cell at Different Exponential Growth Rates. *EcoSal Plus*, 3(1), pp.1–49.

Donachie, W.D., 1968. Relationship between cell size and time of initiation of DNA replication. *Nature*, 219(5158), pp.1077–1079.

Dunlop, M.J. et al., 2008. Regulatory activity revealed by dynamic correlations in gene expression noise. *Nature Genetics*, 40(12), pp.1493–1498.

Elowitz, M.B. et al., 2002. Stochastic gene expression in a single cell. *Science (New York, N.Y.)*, 297(5584), pp.1183–1186.

Eun, Y.-J. et al., 2017. Archaeal cells share common size control with bacteria despite noisier growth and division. *Nature Microbiology*, pp.1–7.

Fantes, P.A., 1977. Control of cell size and cycle time in Schizosaccharomyces pombe. *Journal of cell science*, 24, pp.51–67.

Fantes, P.A. et al., 1975. The regulation of cell size and the control of mitosis. *Journal of Theoretical Biology*, 50(1), pp.213–244.

Ghusinga, K.R., Vargas-Garcia, C.A. & Singh, A., 2016. A mechanistic stochastic framework for regulating bacterial cell division. *Scientific Reports*, 6, p.30229.

Giordano, N. et al., 2016. Dynamical Allocation of Cellular Resources as an Optimal Control Problem: Novel Insights into Microbial Growth Strategies O. A. Igoshin, ed., 12(3), pp.e1004802–28.

Harris, L.K. & Theriot, J.A., 2016. Relative Rates of Surface and Volume Synthesis Set Bacterial Cell Size. *Cell*, 165(6), pp.1479–1492.

Hill, N.S. et al., 2013. A moonlighting enzyme links Escherichia coli cell size with central metabolism. *PLOS Genetics*, 9(7), p.e1003663.

Ho, P.-Y. & Amir, A., 2015. Simultaneous regulation of cell size and chromosome replication in bacteria. *Frontiers in Microbiology*, 6, p.662.

Huls, P.G., Vischer, N.O.E. & Woldringh, C.L., 2018. Different Amounts of DNA in Newborn Cells of Escherichia coli Preclude a Role for the Chromosome in Size Control According to the “Adder” Model. *Frontiers in Microbiology*, 9, p.664.

Iyer-Biswas, S. et al., 2014. Scaling laws governing stochastic growth and division of single bacterial cells. *Proceedings of the National Academy of Sciences*, 111(45), pp.15912–15917.

Jun, S. et al., 2018. Fundamental principles in bacterial physiology-history, recent progress, and the future with focus on cell size control: a review. *Reports on progress in physics. Physical Society (Great Britain)*, 81(5), p.056601.

Kennard, A.S. et al., 2016. Individuality and universality in the growth-division laws of single E. coli cells. *Physical Review E*, 93(1), p.012408.

Kiviet, D.J. et al., 2014. Stochasticity of metabolism and growth at the single-cell level. *Nature*, 514(7522), pp.376–379.

Kleijn, I.T., Krah, L.H.J. & Hermsen, R., 2018. Noise propagation in an integrated model of bacterial gene expression and growth. *PLoS computational biology*, 14(10), p.e1006386.

Klumpp, S. & Hwa, T., 2014. Bacterial growth: global effects on gene expression, growth feedback and proteome partition. *Current opinion in biotechnology*, 28, pp.96–102.

Levine, E. & Hwa, T., 2007. Stochastic fluctuations in metabolic pathways. *Proceedings of the National Academy of Sciences of the United States of America*, 104(22), pp.9224–9229.

Liao, C., Blanchard, A.E. & Lu, T., 2017. An integrative circuit-host modelling framework for predicting synthetic gene network behaviours. *Nature Microbiology*, 403, p.339.

Logsdon, M.M. et al., 2017. A Parallel Adder Coordinates Mycobacterial Cell- Cycle Progression and Cell-Size Homeostasis in the Context of Asymmetric Growth and Organization. *Current Biology*, pp.1–16.

Maitra, A. & Dill, K.A., 2015. Bacterial growth laws reflect the evolutionary importance of energy efficiency. *Proceedings of the National Academy of Sciences*, 112(2), pp.406–411.

Maitra, A. & Dill, K.A., 2016. Modeling the Overproduction of Ribosomes when Antibacterial Drugs Act on Cells. *Biophysical journal*, 110(3), pp.743–748.

Marr, A.G., 1991. Growth rate of Escherichia coli. *Microbiological reviews*, 55(2), pp.316–333.

Micali, G. et al., 2018. Concurrent processes set E. coli cell division. *Science Advances*, 4(11), p.eaau3324.

Molenaar, D. et al., 2009. Shifts in growth strategies reflect tradeoffs in cellular economics. *Molecular Systems Biology*, 5(1), p.323.

Monds, R.D. et al., 2014. Systematic perturbation of cytoskeletal function reveals a linear scaling relationship between cell geometry and fitness. *Cell reports*, 9(4), pp.1528–1537.

Palacios, P., Vicente, M. & Sánchez, M., 1996. Dependency of Escherichia coli cell-division size, and independency of nucleoid segregation on the mode and level of ftsZ expression. *Molecular microbiology*, 20(5), pp.1093–1098.

Pandey, P.P. & Jain, S., 2016. Analytic derivation of bacterial growth laws from a simple model of intracellular chemical dynamics. *Theory in biosciences = Theorie in den Biowissenschaften*, pp.1–10.

Pandey, P.P., Singh, H. & Jain, S., 2018. Exponential trajectories, cell size fluctuations and the adder property in bacteria follow from simple chemical dynamics and division control. *biorxiv.org*

Priestman, M. et al., 2017. Mycobacteria Modify Their Cell Size Control under Sub-Optimal Carbon Sources. *Frontiers in Cell and Developmental Biology*, 5, p.64.

Reuveni, S., Ehrenberg, M. & Paulsson, J., 2017. Ribosomes are optimized for autocatalytic production. *Nature*, 547(7663), pp.293–297.

Schaechter, M., Maaloe, O. & Kjeldgaard, N.O., 1958. Dependency on medium and temperature of cell size and chemical composition during balanced grown of Salmonella typhimurium. *Journal of general microbiology*, 19(3), pp.592–606.

Scott, M. et al., 2014. Emergence of robust growth laws from optimal regulation of ribosome synthesis. *Molecular Systems Biology*, 10, p.747.

Scott, M. et al., 2010. Interdependence of cell growth and gene expression: origins and consequences. *Science (New York, N.Y.)*, 330(6007), pp.1099–1102.

Sharma, P., Pandey, P.P. & Jain, S., 2018. Modeling the cost and benefit of proteome regulation in a growing bacterial cell. *Physical biology*, pp.1–15.

Si, F. et al., 2017. Invariance of Initiation Mass and Predictability of Cell Size in Escherichia coli. *Current biology : CB*, 27(9), pp.1278–1287.

Si, F. et al., 2018. Mechanistic origin of cell-size control and homeostasis in bacteria. *biorxiv.org*

Sobol, I.M., 1967. On the distribution of points in a cube and the approximate evaluation of integrals. *USSR Computational Mathematics and Mathematical Physics*.

Soifer, I., Robert, L. & Amir, A., 2016. Single-Cell Analysis of Growth in Budding Yeast and Bacteria Reveals a Common Size Regulation Strategy. *Current Biology*, 26(3), pp.356–361.

Taheri-Araghi, S., Bradde, S., et al., 2015. Cell-size control and homeostasis in bacteria. *Current biology : CB*, 25(3), pp.385–391.

Taheri-Araghi, S., Brown, S.D., et al., 2015. Single-Cell Physiology. *Annual Review of Biophysics*, 44, pp.123–142.

Thomas, P. et al., 2018. Sources, propagation and consequences of stochasticity in cellular growth. *Nature communications*, 9(1), p.4528.

Turner, J.J., Ewald, J.C. & Skotheim, J.M., 2012. Cell size control in yeast. *Current biology : CB*, 22(9), pp.R350–9.

Vadia, S. & Levin, P.A., 2015. Growth rate and cell size: a re-examination of the growth law. *Current opinion in microbiology*, 24, pp.96–103.

Varsano, G., Wang, Y. & Wu, M., 2017. Probing Mammalian Cell Size Homeostasis by Channel-Assisted Cell Reshaping. *Cell reports*, 20(2), pp.397–410.

Wallden, M. et al., 2016. The Synchronization of Replication and Division Cycles in Individual E. coli Cells. *Cell*, 166(3), pp.729–739.

Wang, P. et al., 2010. Robust growth of Escherichia coli. *Current biology : CB*, 20(12), pp.1099–1103.

Weisse, A.Y. et al., 2015. Mechanistic links between cellular trade-offs, gene expression, and growth. *Proceedings of the National Academy of Sciences*, 112(9), pp.E1038–47.

Zheng, H. et al., 2016. Interrogating the Escherichia coli cell cycle by cell dimension perturbations. *Proceedings of the National Academy of Sciences*, p.201617932.